

# Responses of water use efficiency to phenology in typical subtropical forest ecosystems—A case study in Zhejiang Province

Fengsheng GUO<sup>1,2</sup>, Jiaxin JIN<sup>1,2\*</sup>, Bin YONG<sup>1,2</sup>, Ying WANG<sup>3</sup> & Hong JIANG<sup>4</sup><sup>1</sup> State Key Laboratory of Hydrology-Water Resources and Hydraulic Engineering, Hohai University, Nanjing 210098, China;<sup>2</sup> School of Earth Sciences and Engineering, Hohai University, Nanjing 211100, China;<sup>3</sup> School of Culture Industry and Tourism Management, Sanjiang University, Nanjing 210012, China;<sup>4</sup> International Institute for Earth System Science, Nanjing University, Nanjing 210023, China

Received October 2, 2018; revised April 8, 2019; accepted April 15, 2019; published online May 20, 2019

**Abstract** Ecosystem-scale water-use efficiency (WUE) is an important indicator for understanding the intimately coupled relationship between carbon and water cycles in ecosystems. Previous studies have suggested that both abiotic and biotic factors have significant effects on WUE in forest ecosystems. However, responses of WUE to phenology in the context of climate change remain poorly understood. In this study, we analyzed the sensitivity and response patterns of seasonal WUE to phenology in Zhejiang Province where typical subtropical forest ecosystems are located, and discussed potential causes of the changes of the sensitivity and response patterns along different climate gradient during 2000–2014. The results of interannual partial correlation analysis showed widespread negative correlations between WUE and the start of growing season (SOS) in spring. This is because the increase in gross primary product (GPP) is larger than that of evapotranspiration (ET), resulting from an advanced SOS. The positive correlation between WUE and SOS was widely observed in summer mainly because of water stress and plant ecological strategy. The autumn WUE enhanced with the delay in the end of growing season (EOS) mainly because of the increase in GPP meanwhile the decrease or steadiness in ET, resulting from a delayed EOS. In space, the sensitivity of spring WUE to SOS significantly decreased along the radiation gradient, which might be related to strong soil evaporation in high radiation area; the sensitivity of WUE to SOS in summer showed a positive correlation with precipitation and a negative correlation with temperature, respectively, which might be attributed to the compensation of GPP to the delayed SOS and water stress caused by high temperature. The sensitivity of WUE to EOS increased significantly along the radiation and precipitation gradients in autumn, which may be because the increase of radiation and precipitation provides more water and energy for photosynthesis.

**Keywords** Water-use efficiency, Gross primary product, Evapotranspiration, Phenology, Climate gradient, Forest

**Citation:** Guo F, Jin J, Yong B, Wang Y, Jiang H. 2020. Responses of water use efficiency to phenology in typical subtropical forest ecosystems—A case study in Zhejiang Province. *Science China Earth Sciences*, 63: 145–156, <https://doi.org/10.1007/s11430-018-9360-0>

## 1. Introduction

As a core of energy and material cycles in terrestrial ecosystems, the carbon-water coupling cycle of terrestrial ecosystems is a key scientific issue of ecosystem function (Liu et al., 2018; Li et al., 2019). Water-use efficiency (WUE) is an

important indicator for understanding the intimately coupled relationship between carbon and water cycles in terrestrial ecosystems, which is being greatly concerned by plant physiology and ecology (Le Houerou, 1984; Reichstein et al., 2010; Huang et al., 2015; Guerrieri et al., 2016; Liu et al., 2019). The definition of WUE varies at different levels or scales (Beer et al., 2009; Ponton et al., 2010; Zhou et al., 2014). At the ecosystem scale, WUE is widely defined as the

\* Corresponding author (email: [jjaxinking@hhu.edu.cn](mailto:jjaxinking@hhu.edu.cn))

ratio between gross primary productivity (GPP) and evapotranspiration (ET) (Reichstein et al., 2010; Huang et al., 2015; Guerrieri et al., 2016), which indicates the rate of carbon uptake per unit of water lost and integrates the comprehensive response of vegetation composition and evaporation in ecosystem (Law et al., 2002; Keenan et al., 2013; Tang et al., 2015; Huang et al., 2017). Recently, global climate has significantly changed (Wolf et al., 2016), and it is valuable to reveal the spatio-temporal variability of WUE in ecosystems for predicting and dealing with the impacts of future climate change on carbon and water cycles (Yang et al., 2014).

Plant phenology is timing of events within plant life cycle or state-transitions of ecological processes, such as the sprout of deciduous plants and the turning point of evergreen leaves from dormancy to photosynthesis. From individual plants to ecosystems, many processes are directly or indirectly regulated by phenology, especially those related to carbon (e.g., photosynthesis and respiration) and water (e.g., transpiration and evaporation) cycles (Morissette et al., 2009; Reed et al., 2009).

Studies have shown that phenology is very sensitive to climate change, and interannual variations of phenology are consistent with interannual variations of climates during the growing season (Piao et al., 2015; Ge et al., 2016; Dai et al., 2017; Wang et al., 2015, 2017; Richardson et al., 2013). Therefore, the variations of climates could affect phenology, and consequently the process and intensity of vegetation physiological activity will also be affected. For example, in early spring, an earlier sprout or leaf recovery means that vegetation enters the growth stage earlier. Then GPP will increase at the beginning of the growing season (Richardson et al., 2010; Jin et al., 2017b). Meanwhile, a larger leaf area will also increase plant transpiration and reduce soil evaporation (Beer et al., 2009; McPherson, 2007; Shen et al., 2015). Further, these changes of GPP and ET will result in abnormal fluctuations of ecosystem WUE. However, to this day, our knowledge on regulations of biotic factors (e.g., phenology) on WUE in the context of climate change is still not that clear.

Considering the importance of phenology and climate change on WUE, we focused on the forest ecosystem in Zhejiang Province, where the subtropical forest are typical, and used remote sensing data to detect interannual variations of WUE and phenology. Furthermore, we analyzed the sensitivity and response pattern of WUE to phenology, and clarified their variations along climatic gradients. Finally, we tried to find the potential causes of the difference between the responses of seasonal WUE to phenology along climate gradients. This work will help us to deepen the understanding of the biological regulatory mechanisms of carbon-water coupling cycle and improve the ability of carbon-water cycle prediction in subtropical forest ecosystem.

## 2. Study area and data

### 2.1 Study area

Zhejiang Province is located at the southeastern coast of China and the southern flank of the Yangtze River Delta. It ranges from about 27°N to 31°N and 118°E to 123°E (Figure 1). It belongs to a typical subtropical monsoon climate with four distinct seasons and abundant sunshine and heat. The annual average temperature is 15–18°C and the average hours of illumination is 4.6–5.8 h per day. In the past 60 years, the temperature in Zhejiang Province has been increasing while the rainfall has been decreasing, and the climate is becoming “hot and dry”. The forest coverage rate of Zhejiang Province is 61.17%. The forest vegetation includes evergreen broad-leaved forest, deciduous broad-leaved forest, and evergreen and deciduous broad-leaved mixed forest. Considering the local climate change and abundant natural resources, it is of great significance to study the interactions between the WUE and phenology in forest ecosystems in Zhejiang Province.

### 2.2 MODIS GPP and ET data

Remote sensing data have the advantages of long time span and wide range for the study of ecosystem WUE (Tang et al., 2015; Sun et al., 2016). MODIS GPP (MOD17) and ET (MOD16) data with a 0.05° spatial resolution from 2000 to 2014 were used in this study (<http://www.nts.gov.cn/>), and the unit of GPP and ET is  $\text{g C m}^{-2}$  and mm, respectively. MODIS GPP and ET were derived from satellite-based vegetation information data and meteorological data, using the approach of the light-use efficiency model and the Penman-Monteith method, respectively. More details of the data were provided in Running et al. (2004), Zhao et al. (2005) and Mu et al. (2011). Based on the monthly data of GPP and ET, the seasonal mean values of GPP and ET were calculated, which were used to obtain the seasonal ecosystem-scale WUE. The seasons in our analysis include spring, summer and autumn, defined as March-May, June-August and September-November, respectively.

### 2.3 Meteorological data

The meteorological data concerned include near-surface temperature (°C), precipitation rate ( $\text{mm h}^{-1}$ ) and short-wave solar radiation ( $\text{MJ m}^{-2} \text{day}^{-1}$ ). They were derived from China Meteorological Forcing Dataset ([westdc.westgis.ac.cn/data/](http://westdc.westgis.ac.cn/data/)), with a temporal resolution of three-hour and a spatial resolution of 0.1°. It's a set of reanalysis dataset of near-surface meteorological and environmental elements developed by Institute of Qinghai-Tibet Plateau Research. This dataset is based on the international available Princeton reanalysis data, GLDAS data, GEWEX-SRB radiation data,

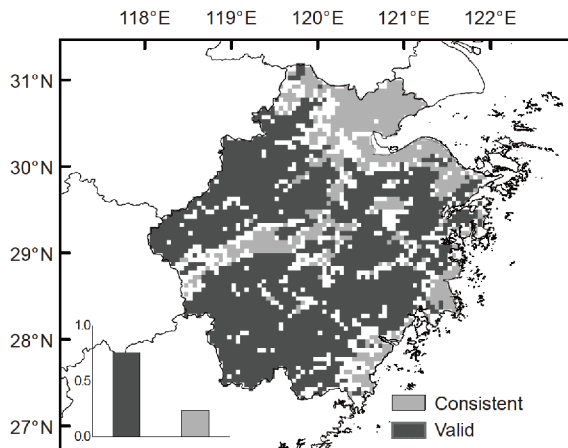


**Figure 1** The vegetation spatial distribution, in which the dark grey pixels are all forest cover pixels from 2001 to 2012, and the light grey pixels are the valid pixels.

and TRMM precipitation data, and composed of the conventional meteorological observation data of the China Meteorological Administration (Chen et al., 2011). In order to match the remote sensing data, the spatial resolution of the climatic data were interpolated from  $0.1^\circ$  to  $0.05^\circ$  by the nearest interpolation.

## 2.4 Land cover type data

The land cover type data used in this study were derived from MODIS land cover type product (MCD12C1) at a spatial resolution of  $0.05^\circ$ , which provides information on land cover type assessment, percentage distribution and quality. It includes data classification products with different classification schemes based on land cover features extracted from Terra. In our study, 17 types of land cover defined by IGBP (International Geosphere-Biosphere Programme) were used, including 11 types of natural vegetation classification, 3 types of mosaic land use, and 3 types of non-vegetated land. The classification came from a supervised decision tree classification method with an accuracy of 75%. In order to reduce the uncertainty that WUE varies at different land cover types, the forest pixels were included in further study according to the land cover type data of Zhejiang Province from 2001 to 2012, of which the land cover type had no change during the twelve years.

## 3. Methods

### 3.1 Data preprocessing

Due to the influence of weather, such as clouds, snow and rainfall, and other noises, some data with low quality would result in uncertainty of results. For this study, the valid pixels of the study area were identified according to the following

criteria: (1) The PFT was identified as forest and were constant during 2001–2012; (2) summer active forest ecosystems, of which the summer GPP (from June to August) is the highest and the winter GPP (from December to February) is the lowest during a whole year, were selected; (3) the valid GPP data records should be more than 80% of the total records of each year. Above conditions will make the analysis of the follow-up results of this study more accurate and scientific.

### 3.2 Determination of phenology

Different from the traditional vegetation phenology, the “phenology” captured by satellite-based data represents the transition date of a mixed area rather than an individual plant. There are many methods for extracting vegetation phenology at the regional scale using remote sensing satellite data. The dynamic threshold method was used in this study to derive the phenology because it can be less affected by the type of land cover and obtain more targeted phenological indicators. The daily GPP data was derived from the time series of GPP at a resolution of 8-day using the linear interpolation. Then, the daily GPP was smoothed by singular spectrum analysis (SSA). The SSA approach is allowed for extracting the phenological transition dates (Keenan et al., 2014). This study selected the transitions in spring and autumn based on GPP data during photosynthesis cycle, termed SOS and EOS, respectively. As a typical subtropical forest ecosystem, although the seasonal change of the forest in the area is not obvious, the phenology of “carbon flux” of plants could be still captured based on GPP data, which represents the transformation of plant carbon assimilation capacity rather than vegetation greenness of the forest (Wu et al., 2012, 2013).

### 3.3 Statistical analysis

In this study, linear regression analysis was used to analyze the trend of seasonal WUE and phenology. After controlling the climatic factors (temperature, precipitation rate and radiation), partial correlation analysis was used to analyze the relationship between seasonal WUE and phenology. According to the relationships between WUE, GPP, ET and phenology, six response patterns of WUE to phenology were identified (Jin et al., 2017a). Furthermore, the climate gradients were established on the multi-year average of climate at the level of pixels, and variations in the sensitivities of WUE to phenology were detected along the climatic gradients. In order to reduce the interference of outliers, Theil-Sen’s slope and Mann-Kendall test were used to analyze relationships between the interannual variations of WUE and phenology and relationships between the sensitivity of WUE

to phenology and climate gradients (Wang et al., 2018).

## 4. Results

### 4.1 Spatio-temporal variations in WUE and phenology

Figure 2 shows the spatial distribution of the interannual variations of the mean seasonal WUE, SOS and EOS in the study area from 2000 to 2014. Overall, spring WUE increased with an average annual value of  $0.0024 \pm 0.0038 \text{ g C m}^{-2} \text{ mm}^{-1}$ , and 9.79% of valid pixels were significant. Among them, 75.48% of the valid pixels showed an annual increase of  $0.0059 \pm 0.0028 \text{ g C m}^{-2} \text{ mm}^{-1} \text{ yr}^{-1}$ , and 24.52% of the valid pixels showed a decreasing trend at a rate of  $0.0024 \pm 0.0023 \text{ g C m}^{-2} \text{ mm}^{-1} \text{ yr}^{-1}$ . Specifically, the areas where WUE decreased were mainly in the northwest forests and the forests between  $29^\circ\text{N}$  and  $30^\circ\text{N}$  (Figure 2a). Compared to the result of spring, the summer WUE also increased with 9.31% significant trends, but the proportion of pixels of increasing WUE in summer (66.91% of valid pixels) was less than that in spring. Nevertheless, the overall increasing magnitude of WUE in summer ( $0.0058 \pm 0.0028 \text{ g C m}^{-2} \text{ mm}^{-1} \text{ yr}^{-1}$ ) was greater than that in spring (Figure 2b). Different from spring and summer, a large-scale (94.36% of the valid pixels) negative trend, with a value of  $0.0066 \pm 0.004 \text{ g C m}^{-2} \text{ mm}^{-1}$ , was found for autumn WUE, of which 27.67% were statistically significant and the magnitude was greater than that in spring and summer (Figure 2c).

Overall, the trends of SOS ranged from  $-0.66$  to  $1.17 \text{ day yr}^{-1}$ , 76.92% of which showed SOS delay, with an average of  $2.3 \pm 1.7$  days per decade. The remaining pixels showed an advanced SOS, with an average value of  $1.5 \pm 1.4$  days per decade, mainly distributed in the southwest of the region (Figure 2d). However, only 4.68% of valid pixels were statistically significant. The interannual regression coefficients of EOS ranged from  $-1.01$  to  $0.48 \text{ day yr}^{-1}$ , with 11.54% of valid pixels being statistically significant, and the advance and delay in EOS were distributed throughout the study area. The delay in EOS occurred in 35.71% of the valid pixels, with an average value of  $1.0 \pm 2.1$  days per decade, which may be related to the delay of SOS (Fu et al., 2014; Keenan and Richardson, 2015; Liu et al., 2016). The advance in EOS occurred in the remaining pixels, with an average value of  $2.4 \pm 0.9$  days per decade, mainly located in the eastern of the region.

Figure 3 shows the spatial change of WUE trend in different seasons under phenological changes during 2000–2014. The horizontal axis is the interannual linear trend of phenology and the vertical axis is the interannual linear trend of seasonal WUE. Each point in these scatter diagrams represents the average value of the 30 adjacent points from the low to the high value after sorted by the horizontal axis. The interannual trend of spring WUE was negatively correlated

with that of SOS in space (Sen's slope =  $-0.004$ ,  $p < 0.01$ ). That is, the enhancement of WUE in the region with greater advanced SOS was stronger, and WUE in the region with delayed SOS showed a weakly increase or decrease (Figure 3a). Different from spring, the interannual variation of summer WUE was positively correlated with that of SOS (Sen's slope =  $0.0039$ ,  $p < 0.01$ ), that is, the greater the advance of SOS was, the more stable the interannual variation of WUE became (Figure 3b). The result in autumn (Figure 3c) showed that regardless of the delayed or advanced EOS, the overall WUE significantly decreased, and the interannual variations of WUE and EOS were spatially positively correlated (Sen's slope =  $0.0049$ ,  $p < 0.01$ ). The greater the EOS delayed, the weaker the WUE reduction became. In other words, a later EOS will reduce the intensity decline of autumn WUE in forest ecosystems.

### 4.2 The relationship between WUE and phenology

After controlling temperature, precipitation rate and radiation, the partial correlation coefficients between WUE and phenology were calculated by Pearson's partial correlation analysis. Figure 4 shows the spatial distribution of partial correlation coefficients between seasonal WUE and phenological variables. A negative correlation between spring WUE and SOS (Pearson's  $r = -0.2 \pm 0.2$ ) dominated the study area (81.42% of the total valid pixels), and 20.94% of them were statistically significant. The positive correlation coefficient was poor with an average of  $0.1 \pm 0.1$ , mainly located in the northwest of the study area (Figure 4a). Different from spring, the positive relationship between summer WUE and SOS was dominant with an average of  $0.4 \pm 0.2$  (82.43% of valid pixels), and 34.13% of them were significant (Pearson's  $r = 0.3 \pm 0.3$ ). About 17.57% of valid pixels showed a negative correlation, with an average Pearson's partial coefficient of  $-0.3 \pm 0.2$ , which were mainly in the northeast of the study area. In autumn, WUE and EOS generally showed a positive correlation ( $r = 0.3 \pm 0.2$ ), and 34.18% of the valid pixels exhibited significant correlations. About 85.58% of valid pixels showed a positive correlation with an average value of  $0.4 \pm 0.2$ , while the others showed a negative correlation with a low correlation of  $-0.1 \pm 0.1$  (Figure 4c).

In order to investigate the potential impacts of climate change on the biological regulatory of ecosystem-scale WUE, we further analyzed the spatial variation of the sensitivity of seasonal WUE to phenological changes along the climatic gradients (annual mean of temperature, precipitation rate and radiation) (Figure 5). To reduce the disturbance of outliers, the Theil Sen's slope and Mann-Kendall test were used to analyze the relationship between the sensitivity and climate. The results showed that the negative correlation between spring WUE and SOS significantly weakened with the increase of local radiation (Sen's slope =  $0.0059$ ,



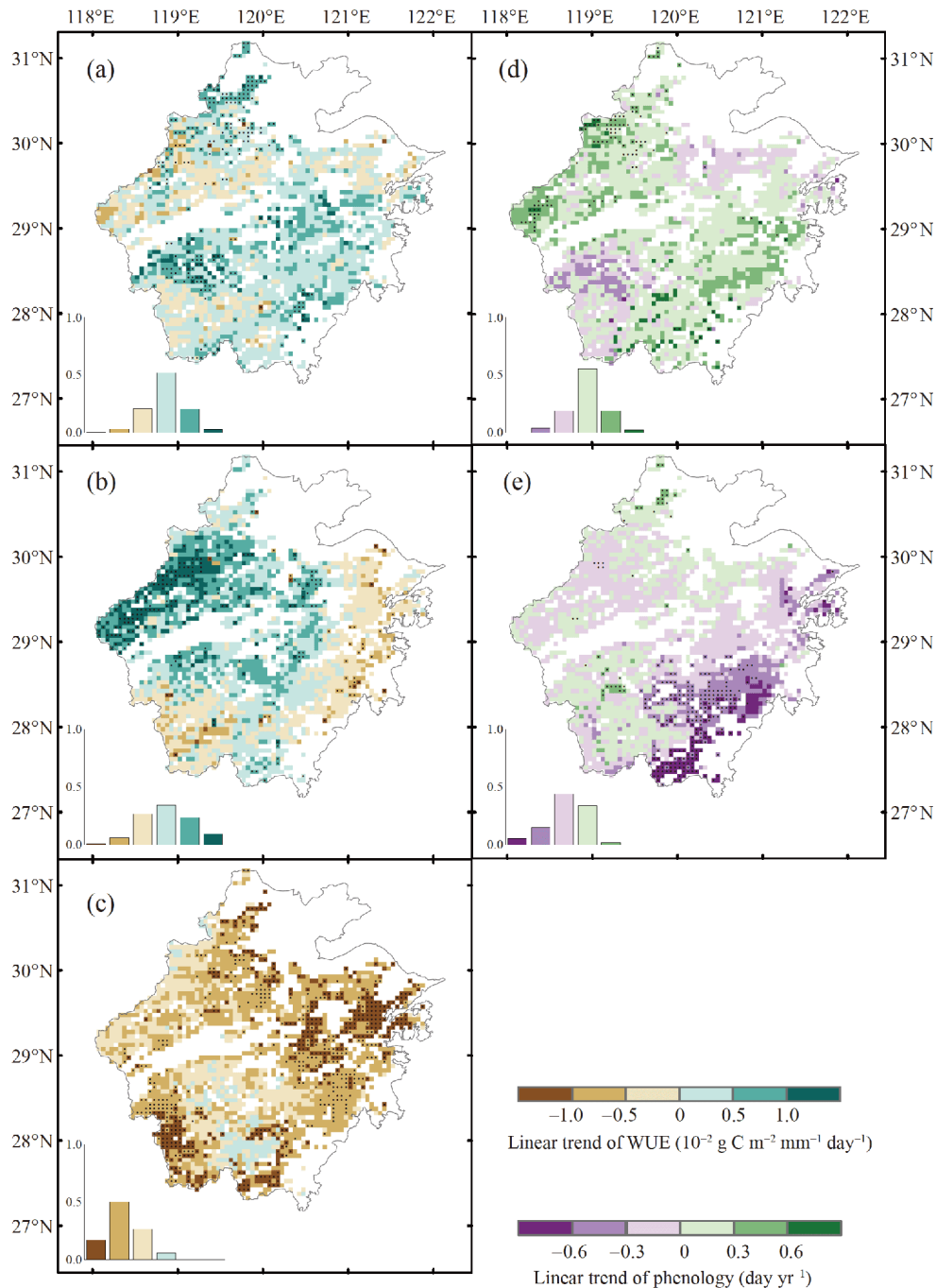


**Figure 2** Spatial distribution of linear trend of seasonal WUE ((a)–(c)), SOS (d) and EOS (e) during 2000–2014. Seasonal WUE are calculated during spring, summer and autumn, respectively. The white areas denote invalid satellite-image pixels. The dotted regions indicate areas where the trends were significant.

$p=0.019$ ). Along the temperature and precipitation gradients, the sensitivity of spring WUE to phenology did not change significantly ( $p>0.05$ ). The positive correlation between summer WUE and SOS was significantly correlated with the gradients in local precipitation and temperature. Specifically, the positive correlation between summer WUE and SOS increased with local precipitation while reduced with local temperature (Sen's slope=1.2528 and  $-0.0452$ , respectively,  $p<0.01$ ). That is, the promotion of a later SOS on summer

WUE was stronger in a higher precipitation but lower temperature region. Along the radiation gradient, there was no significant trend in the sensitivity of WUE to the phenological change. In autumn, the positive correlation between WUE and EOS significantly increased along the precipitation and radiation gradients (Sen's slope =2.8851 and 0.0092, respectively,  $p<0.05$ ). That is, the enhancement of a delayed EOS on WUE was more obvious in areas where both radiation and precipitation were high. However, along the

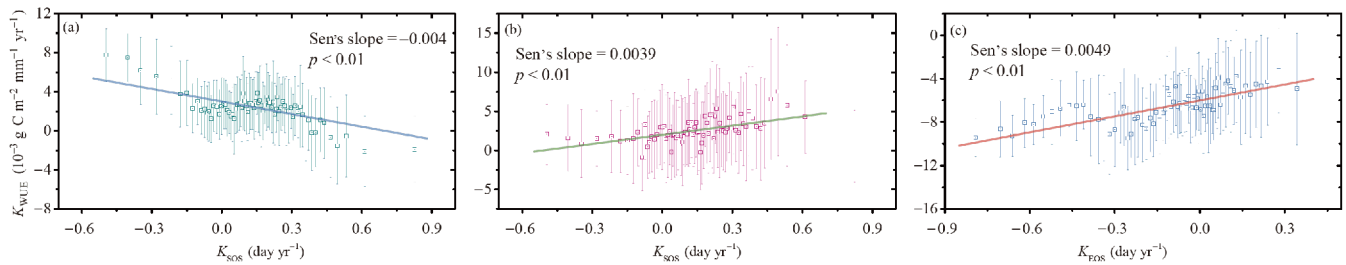


**Figure 3** Relationships between of trends of seasonal WUE and the trends of phenology. Each point in the graph represents the average value of the 30 adjacent points from the low value after sorting by the horizontal axis. The subplots (a)–(c) indicate spring, summer and autumn WUE, respectively.

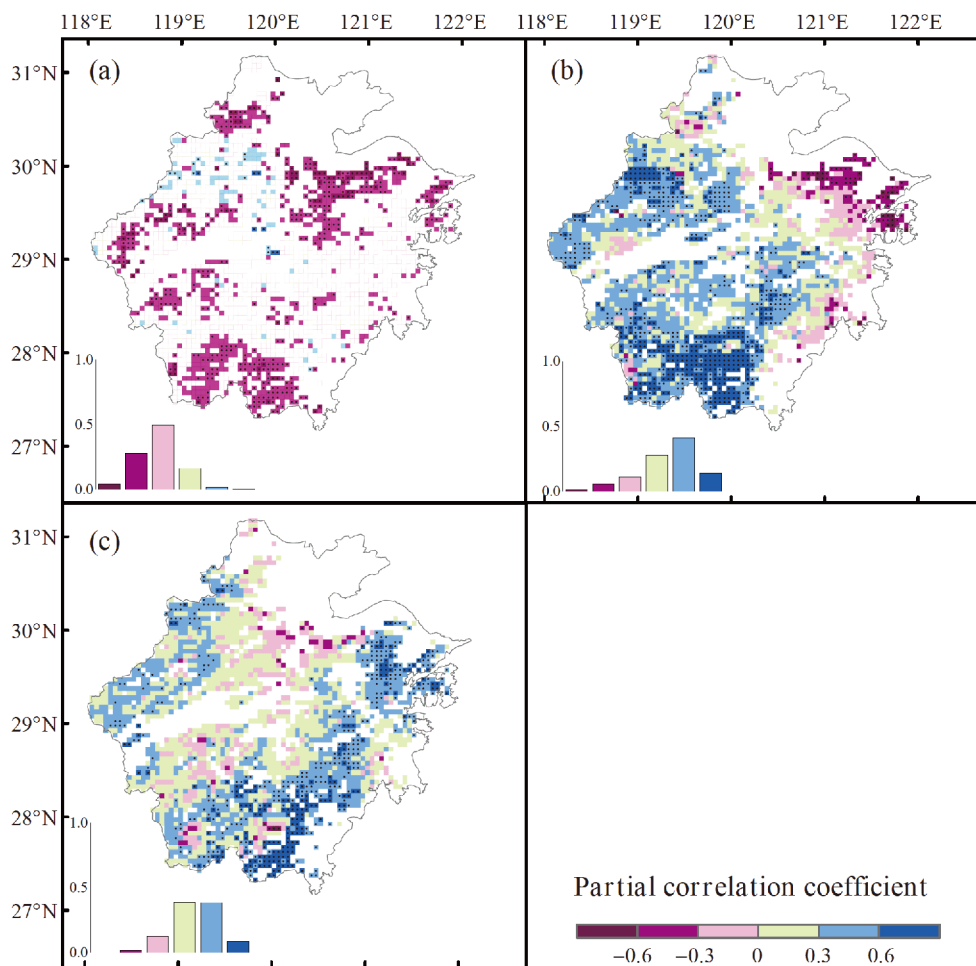


**Figure 4** Spatial distribution of partial correlation coefficients between the phenology (SOS and EOS) and water-use efficiency (WUE) during (a) spring, (b) summer and (c) autumn during 2000–2014. Partial correlation coefficient is calculated by Pearson's partial correlation after controlling the climatic factors (temperature, precipitation and radiation). The white areas denote invalid satellite-image pixels. The dotted regions indicate areas where the trends were significant.

temperature gradient, the Sen's slope was not significant ( $p > 0.05$ ).

### 4.3 Response patterns of WUE to phenology

Responses of WUE to phenology represent the coupled responses of GPP and ET to phenology. The six response patterns of WUE to phenology were identified by the partial

correlation coefficients between WUE, GPP, ET and phenology in spring, summer and autumn, respectively. The spatial distributions are shown in Figure 6.

Pattern VI ( $R_{GPP} < 0$ ,  $R_{ET} < 0$ ,  $R_{WUE} < 0$ ) dominated the response of WUE in spring, accounting for 41.1% of valid pixels, followed by pattern III (20.0%). It indicated that the negative correlation between WUE and SOS in spring was mainly due to the increase of spring GPP with an advanced

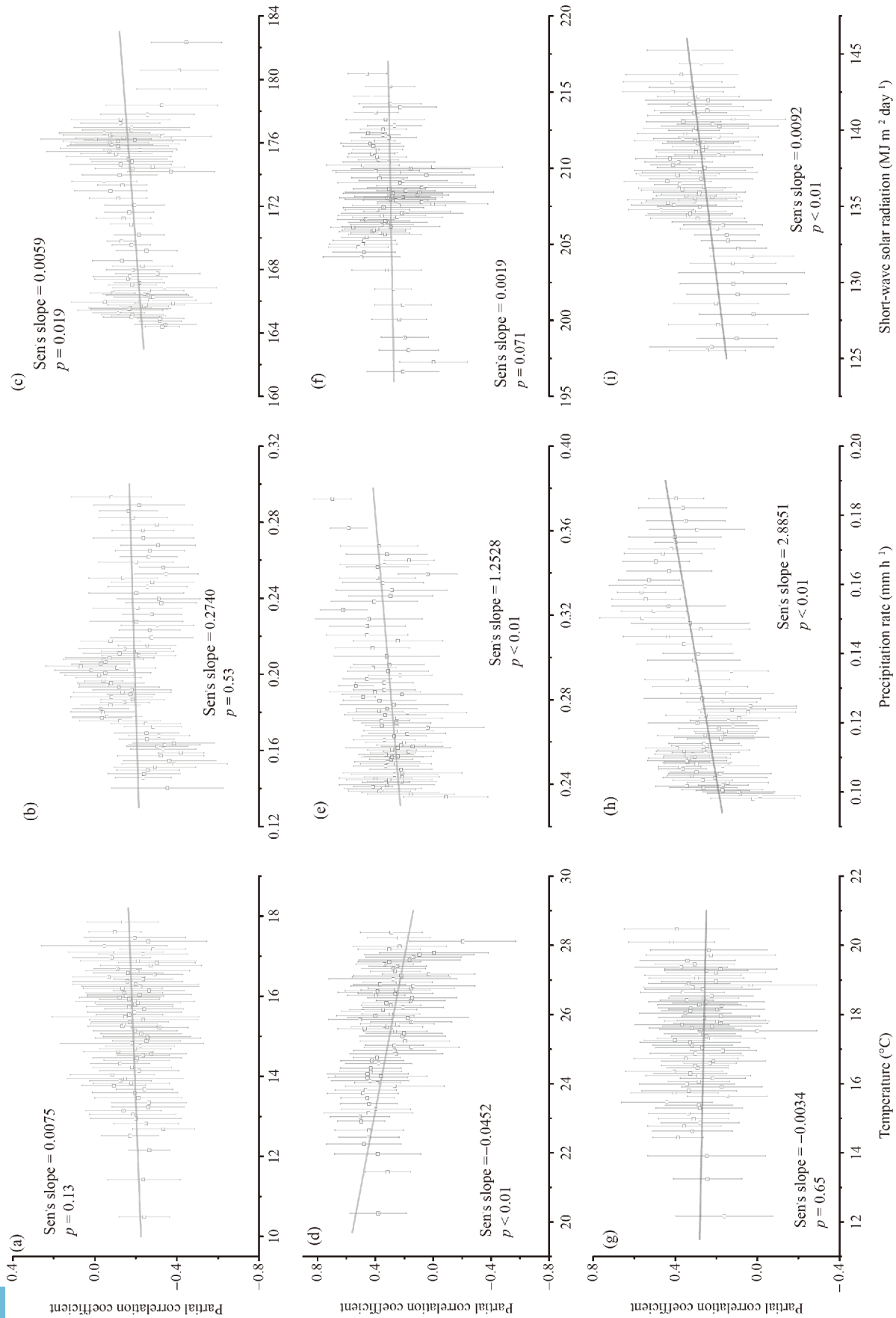


**Figure 5** Spatial variation of sensitivity of seasonal WUE to phenology (SOS and EOS) during (a)-(c) spring; (d)-(f) summer and (g)-(i) autumn with (a), (d), (g) temperature; (b), (e), (h) precipitation and (c), (f), (i) radiation gradients. Sensitivity is expressed by partial correlation coefficient between WUE and SOS/EOS. Data was fitted by Theil Sen's slope and Mann-Kendall test.

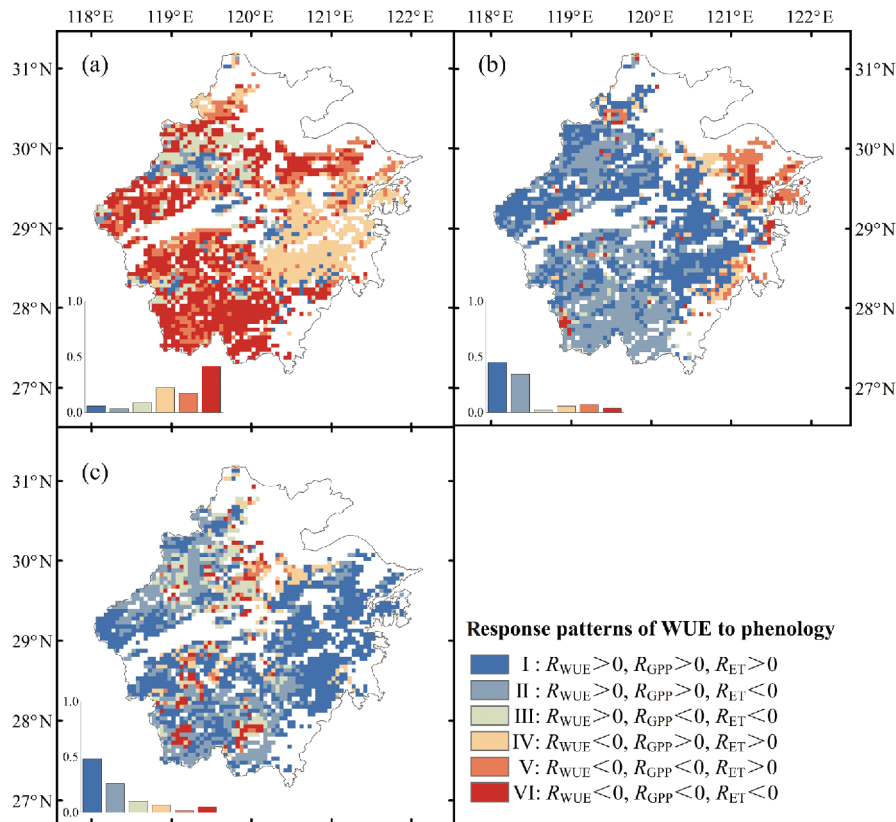


**Figure 6** Spatial distribution of response patterns of seasonal WUE to phenology (SOS and EOS).  $R_{WUE}$ ,  $R_{GPP}$ ,  $R_{ET}$  indicate the partial correlation coefficients of WUE, GPP, ET with the phenology after controlling the climatic factors (including temperature, precipitation, radiation), respectively. (a)–(c) are calculated during spring, summer and autumn, respectively. The white areas denote invalid satellite-image pixels in this study.

SOS. Meanwhile, although ET may also increase with a larger leaf area, the increase in GPP is greater than that of ET (Figure 6a). Figure 6b shows the spatial distribution of response patterns of WUE to SOS in summer, with pattern I and pattern II accounting for 46.7% and 32.6% of valid pixels, respectively. This indicated the positive correlation between WUE and SOS in summer was mainly caused by the two reasons: (1) An earlier SOS led to a lower summer soil moisture, so both the GPP and ET decreased in summer while GPP decreased more strongly than ET; (2) summer GPP decreased with an advanced SOS, while summer ET increased. Both of these two conditions would lead to the decrease of WUE in summer with an earlier SOS. Similar to summer, pattern I and pattern II also dominated autumn, accounting for 49.7% and 28.0% of valid pixels, respectively (Figure 6c). It indicates that an increase in autumn GPP is mainly due to a delayed EOS, which may be related to a longer photosynthetic period. However, the response of autumn ET to EOS is uncertain for a longer transpiration period and a lower surface evaporation due to a delayed EOS. Even if autumn ET increased, the increase of ET is relatively small than that of GPP.

In our study, we further analyzed the spatial variations of response patterns of seasonal WUE to phenological changes along the climatic gradients. The statistics of the response

patterns of WUE to phenology were performed for each 200 pixels from the lowest value, sorted by the average annual climate value of pixels. The results are shown in Figure 7, of which the horizontal axis represents the mean climate of each group, and the vertical axis represents the percentage of each pattern. The results showed that in spring, all temperature intervals were dominated by pattern VI, followed by pattern V and pattern IV. The change of each pattern along the temperature gradient was not obvious. Generally speaking, pattern IV showed a certain downward trend with temperature. Along the precipitation gradient, the response patterns changed significantly. Overall, pattern IV dominated in low precipitation areas, while pattern VI dominated in high precipitation regions. When the precipitation rate was less than 0.22 mm, pattern VI increased with precipitation while pattern IV decreased with precipitation. When the precipitation rate was more than 0.22 mm, pattern IV maintained a low level (about 3%) and pattern VI reached a high level (about 67%). Hence, pattern VI transferred to pattern VI with the increase of precipitation in spring, which indicated that even if SOS advanced, GPP and ET would still decrease if spring rainfall was insufficient. For the radiation gradient, pattern VI was dominant in low radiation areas, and pattern IV was dominant in moderate radiation areas. No obviously dominant pattern was found in high radiation regions.



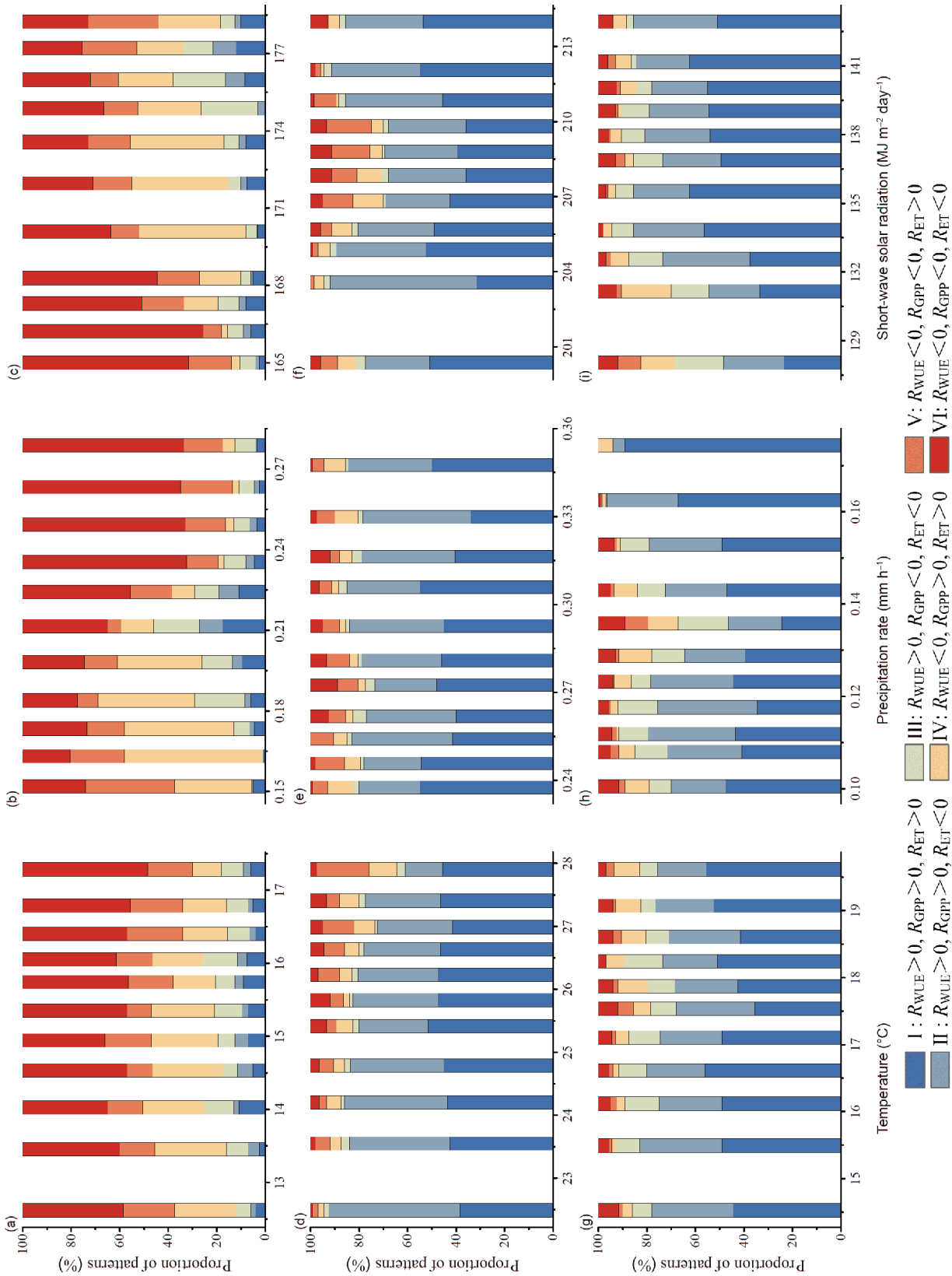


**Figure 7** Spatial variation of response patterns of seasonal WUE to phenological factors (SOS and EOS) during (a)–(c) spring, (d)–(f) summer and (g)–(i) autumn along the (a), (d), (g) temperature, (b), (e), (h) precipitation and (c), (f), (i) radiation gradients. The statistics of response patterns of WUE to phenology was performed for each 200 pixels from the lowest value, sorted by the average annual climate value of pixels.

In summer, pattern I and II largely existed in all temperature intervals. However, along the temperature gradient, pattern II significantly decreased from 54.0% to 15.5%, and gradually transformed into pattern IV and V. Along the precipitation and radiation gradients, the changes of response patterns were not significant. Generally speaking, pattern I and II dominated each interval along the precipitation and radiation gradients.

In autumn, pattern I dominated in all temperature intervals, followed by pattern II. Generally speaking, the percentage of pattern II showed a slight increasing trend along the temperature gradient. Along the precipitation gradient, the response patterns changed significantly. In the low precipitation areas, the proportions of pattern I and II were nearly equal, while in the high precipitation area, pattern I was dominant with the maximum value of 89%. Similar to the result along the precipitation gradient, the WUE response patterns showed that pattern I and II had a high proportion in the low-radiation regions, and pattern I became the dominant pattern in the high-radiation regions. These changes indicate that when EOS delayed, increases in precipitation and radiation will increase GPP, ET and WUE in autumn by providing water and energy for forest ecosystems.

## 5. Discussion

### 5.1 Effects of phenological changes on seasonal WUE

Based on the spatio-temporal variations in seasonal WUE, it showed that WUE in spring and summer exhibited an overall increasing trend, while autumn WUE exhibited a large-scale decreasing trend. Moreover, the decreasing magnitude of autumn WUE was much greater than the sum of the increasing magnitudes of the two seasons. Sun et al. (2018) investigated the variations in WUE over the last three decades in China, and pointed out that the interannual WUE in Zhejiang Province was decreasing. Our study supports this viewpoint and further demonstrates that the main reason for the decline is the large-scale decline of WUE in autumn in this area.

For subtropical forest ecosystems, WUE and SOS were negatively correlated in spring. Given the pattern VI and V, we found that the earlier SOS started in spring, the earlier plants began photosynthesis, resulting in the rapid and longer increase in spring GPP (Luyssaert et al., 2007). Meanwhile, the ET changes in spring were uncertain, because an earlier leaf expansion or a larger leaf area in spring increased plant transpiration but reduced evaporation by decreasing surface temperature and solar radiation (Beer et al., 2009; von Arx et al., 2012; Shen et al., 2015). But  $R_{WUE} > 0$  in pattern V and VI suggested that even if spring ET increased, the increase in ET was smaller than that in GPP, which finally resulted in an increase of spring WUE.

For summer, WUE mainly positively correlated with SOS, which may be related to the response of summer GPP to SOS. On the one hand, an earlier SOS may deplete soil water, resulting in the water stress on vegetation physiological processes in summer (Kljun et al., 2006; Hu et al., 2010), and consequently summer GPP decreased. On the other hand, from the view of carbon economy and ecological strategy, if SOS starts later than the normal years, vegetation will have a stronger carbon sequestration performance in the growing season to ensure normal growth. Both of the above will result in a positive correlation between SOS and summer GPP. From the response pattern of WUE to SOS in summer, the large percentage of pattern I and II further supported the above hypothesis. In autumn, WUE also positively correlated with EOS. This is because the later EOS is, the longer extra photosynthetic period is, and thus autumn GPP increased. However, the autumn temperature and soil moisture were usually low, which could not significantly enhance soil or canopy evaporation. Hence the change of ET in autumn was not significant, resulting in an increase in WUE with a later EOS.

### 5.2 The changes of WUE sensitivity along the climate gradients

According to the sensitivity of WUE to phenology and the spatial variation of response patterns along the climatic gradients, the potential impact factors of climate change on the biological regulatory mechanisms to WUE were further discussed and explained.

The sensitivity of WUE to SOS in spring was positively correlated with local radiation. That is, the higher the local radiation is, the weaker the enhancement of advanced SOS on spring WUE is. Although GPP and ET negatively correlated with SOS in high radiation areas, due to the relatively small canopy leaf area in spring, more radiation could penetrate the canopy to the ground, which promoted soil evaporation and ET and consequently decreased spring WUE.

The sensitivity of summer WUE to SOS significantly correlated with spatial precipitation and temperature. This may be associated with water stress and ecological strategy. The SOS in the study area mainly delayed. Therefore, the compensation effect on carbon gain caused by a relatively short growing season may be the main reason for the positive correlation between summer WUE and SOS. It is known that an early SOS with more water loss will lead to a suppression of summer GPP. Notably, although SOS delayed in the study area, water stress caused by high summer temperature also mainly suppress summer GPP. Therefore, in the areas with low precipitation and high temperature, plants have to preserve water from transpiration leading to stomatal closure and inhibition on photosynthesis. Thus, the compensatory effect with a later SOS will be limited by water stress, which

consequently results in a weak positive correlation between WUE and SOS. In contrast, in the areas with high precipitation and low temperature, the stomata and carbon gain was less stressed by soil moisture. Moreover, the growing season in a lower temperature area is shorter, once the SOS delayed, the plants would enhance summer photosynthesis to ensure growth and development. It is consistent with the results that the percentage of pattern I and II in the low temperature regions was larger than that in the high temperature regions. Given the above cause, summer WUE showed a strong positive correlation with SOS in the areas with high precipitation and low temperature. The sensitivity of summer WUE to SOS slightly varied with the precipitation. The results of gradient analysis showed that the sensitivity of WUE to phenology in typical subtropical forest ecosystems varied with local habitat conditions, which should be taken into account for WUE prediction and carbon budget assessment given the future climatic regime changes.

In autumn, the sensitivity of WUE to EOS significantly varied with precipitation and radiation in space. Specifically, along the precipitation gradient, the enhancement of a delayed EOS on autumn WUE became stronger. Because of evapotranspiration and plant absorption during spring and summer, soil moisture tended to be relatively low in autumn. A delayed EOS means extra days for photosynthesis. Hence, more precipitation can increase soil moisture, and consequently enhance plant physiological activity and extra photosynthesis in autumn, which increased autumn WUE. In addition, a significant increase in percentage of pattern I along the precipitation gradient also provides support for this viewpoint. Similar phenomena were observed along the radiation gradient, indicating that autumn radiation provided energy for plant photosynthesis in the EOS-delayed forest ecosystems (Jin et al., 2017a), which promotes autumn GPP and WUE.

## 6. Conclusions

In this study, we investigated interannual variations in seasonal WUE and phenology and relationships between them in the typical subtropical forest ecosystems of Zhejiang Province. We found that seasonal WUE was closely related to phenology in subtropical evergreen and deciduous broad-leaved mixed forest. Meanwhile, the sensitivities of WUE to phenology in different seasons corresponded to different dominant climatic factors and varied with them. The sensitivity of spring WUE to SOS enhanced significantly along the radiation gradient. The sensitivity of summer WUE to SOS in low temperature and high precipitation regions was stronger than that in high temperature and low precipitation areas. The sensitivity of autumn WUE to EOS varied significantly with precipitation and radiation gradient, and it was stronger in high radiation and high precipitation areas. In

summary, we argue that climate change will alert the sensitivity of WUE to phenology, and for subtropical evergreen and deciduous broad-leaved mixed forest, it is necessary to take the biological regulatory mechanisms of WUE under different climate scenarios and local habitat conditions into account when setting parameters for future ecosystem process models and assessing carbon budget.

**Acknowledgements** This work was supported by the National Key R & D Program of China (Grant No. 2018YFA0605402), the National Natural Science Foundation of China (Grant Nos. 41601442 & 41807173), and the Fundamental Research Funds for the Central Universities (Grant No. 2017B06814).

## References

- Beer C, Ciais P, Reichstein M, Baldocchi D, Law B E, Papale D, Soussana J F, Ammann C, Buchmann N, Frank D, Gianelle D, Janssens I A, Knohl A, Köstner B, Moors E, Rouspard O, Verbeeck H, Vesala T, Williams C A, Wohlfahrt G. 2009. Temporal and among-site variability of inherent water use efficiency at the ecosystem level. *Glob Biogeochem Cycle*, 23: GB2018
- Chen Y Y, Yang K, He J, Qin J, Shi J C, Du J Y, He Q. 2011. Improving land surface temperature modeling for dry land of China. *J Geophys Res*, 116: D20104
- Dai J H, Xu Y J, Wang H J, Alatalo J, Tao Z X, Ge Q S. 2017. Variations in the temperature sensitivity of spring leaf phenology from 1978 to 2014 in Mudanjiang, China. *Int J Biometeorol*, 63: 569–577
- Fu Y S H, Campioli M, Vitasse Y, De Boeck H J, Van den Berge J, AbdElgawad H, Asard H, Piao S, Deckmyn G, Janssens I A. 2014. Variation in leaf flushing date influences autumnal senescence and next year's flushing date in two temperate tree species. *Proc Natl Acad Sci USA*, 111: 7355–7360
- Ge Q S, Dai J H, Cui H J, Wang H J. 2016. Spatiotemporal variability in start and end of growing season in china related to climate variability. *Remote Sens*, 8: 433
- Guerrieri R, Lepine L, Asbjornsen H, Xiao J, Ollinger S V. 2016. Evapotranspiration and water use efficiency in relation to climate and canopy nitrogen in U.S. forests. *J Geophys Res-Biogeosci*, 121: 2610–2629
- Huang G, Li Y, Mu X H, Zhao H M, Cao Y F. 2017. Water-use efficiency in response to simulated increasing precipitation in a temperate desert ecosystem of Xinjiang, China. *J Arid Land*, 9: 823–836
- Huang M T, Piao S L, Sun Y, Philippe C, Cheng L, Mao J F, Ben P, Shi X Y, Zeng Z Z, Wang Y P. 2015. Change in terrestrial ecosystem water-use efficiency over the last three decades. *Glob Change Biol*, 21: 2366–2378
- Hu J, Moore D J P, Burns S P, Monson R K. 2010. Longer growing seasons lead to less carbon sequestration by a subalpine forest. *Glob Change Biol*, 16: 771–783
- Jin J X, Wang Y, Zhang Z F, Magliulo V, Jiang H, Cheng M. 2017a. Phenology plays an important role in the regulation of terrestrial ecosystem water-use efficiency in the northern hemisphere. *Remote Sens*, 9: 664
- Jin J X, Zhan W F, Wang Y, Gu B, Wang W, Jiang H. 2017b. Water use efficiency in response to interannual variations in flux-based photosynthetic onset in temperate deciduous broadleaf forests. *Ecol Indic*, 79: 122–127
- Keenan T F, Hollinger D Y, Bohrer G, Dragoni D, Munger J W, Schmid H P, Richardson A D. 2013. Increase in forest water-use efficiency as atmospheric carbon dioxide concentrations rise. *Nature*, 499: 324–327
- Keenan T F, Gray J, Friedl M A, Toomey M, Bohrer G, Hollinger D Y, Munger J W, O'Keefe J, Schmid H P, Wing I S, Yang B, Richardson A D. 2014. Net carbon uptake has increased through warming-induced changes in temperate forest phenology. *Nat Clim Change*, 4: 598–604

- Keenan T F, Richardson A D. 2015. The timing of autumn senescence is affected by the timing of spring phenology: Implications for predictive models. *Glob Change Biol*, 21: 2634–2641
- Kljun N, Black T A, Griffis T J, Barr A G, Gaumont-Guay D, Morgenstern K, McCaughey J H, Nesic Z. 2006. Response of net ecosystem productivity of three boreal forest stands to drought. *Ecosystems*, 9: 1128–1144
- Law B E, Falge E, Gu L, Baldocchi D D, Bakwin P, Berbigier P, Davis K, Dolman A J, Falk M, Fuentes J D, Goldstein A, Granier A, Grelle A, Hollinger D, Janssens I A, Jarvis P, Jensen N O, Katul G, Mahli Y, Matteucci G, Meyers T, Monson R, Munger W, Oechel W, Olson R, Pilegaard K, Paw U K T, Thorgeirsson H, Valentini R, Verma S, Vesala T, Wilson K, Wofsy S. 2002. Environmental controls over carbon dioxide and water vapor exchange of terrestrial vegetation. *Agric For Meteorol*, 113: 97–120
- Le Houerou H N. 1984. Rain use efficiency: A unifying concept in arid-land ecology. *J Arid Environ*, 7: 213–247
- Li Y, Li C H, Xie J B, Liu Y, Liu X C, Wang Y G. 2019. Accumulation of organic carbon and its association with macro-aggregates during 100 years of oasis formation. *Catena*, 172: 770–780
- Liu R, Li Y, Wang Y G, Ma J, Cieraad E. 2019. Variation of water use efficiency across seasons and years: Different role of herbaceous plants in desert ecosystem. *Sci Total Environ*, 647: 827–835
- Liu R, Wang Y G, Li C H, Ma J, Li Y. 2018. Partitioning water source and sinking process of a groundwater-dependent desert plant community. *Plant Soil*, 430: 73–85
- Liu Q, Fu Y S H, Zhu Z C, Liu Y W, Liu Z, Huang M T, Janssens I A, Piao S L. 2016. Delayed autumn phenology in the northern hemisphere is related to change in both climate and spring phenology. *Glob Change Biol*, 22: 3702–3711
- Luyssaert S, Janssens I A, Sulkava M, Papale D, Dolman A J, Reichstein M, Hollmén J, Martin J G, Suni T, Vesala T, Loustau D, Law B E, Moors E J. 2007. Photosynthesis drives anomalies in net carbon-exchange of pine forests at different latitudes. *Glob Change Biol*, 13: 2110–2127
- McPherson R A. 2007. A review of vegetation—Atmosphere interactions and their influences on mesoscale phenomena. *Prog Phys Geogr*, 31: 261–285
- Morissette J T, Richardson A D, Knapp A K, Fisher J I, Graham E A, Abatzoglou J, Wilson B E, Breshears D D, Henebry G M, Hanes J M, Liang L. 2009. Tracking the rhythm of the seasons in the face of global change: Phenological research in the 21st century. *Front Ecol Environ*, 7: 253–260
- Mu Q, Zhao M, Running S W. 2011. Improvements to a modis global terrestrial evapotranspiration algorithm. *Remote Sens Environ*, 115: 1781–1800
- Piao S L, Tan J G, Chen A P, Fu Y S H, Philippe C, Liu Q, Janssens I A, Sara V, Zeng Z Z, Jeong S J L Y, Myneni R B, Peng S S, Shen M G, Peñuelas J. 2015. Leaf onset in the northern hemisphere triggered by daytime temperature. *Nat Commun*, 6: 6911
- Ponton S, Flanagan L B, Alstad K P, Johnson B G, Morgenstern K, Kljun N, Black T A, Barr A G. 2010. Comparison of ecosystem water-use efficiency among Douglas-fir forest, aspen forest and grassland using eddy covariance and carbon isotope techniques. *Glob Change Biol*, 12: 294–310
- Reed B C, Schwartz M D, Xiao X. 2009. *Phenology of Ecosystem Processes*. New York: Springer
- Reichstein M, Ciais P, Papale D, Valentini R, Running S, Viovy N, Cramer W, Granier A, Ogée J, Allard V, Aubinet M, Bernhofer C, Buchmann N, Carrara A, Grünwald T, Heimann M, Heinesch B, Knohl A, Kutsch W, Loustau D, Manca G, Matteucci G, Miglietta F, Ourcival J M, Pilegaard K, Pumpanen J, Rambal S, Schaphoff S, Seufert G, Soussana J F, Sanz M J, Vesala T, Zhao M. 2010. Reduction of ecosystem productivity and respiration during the european summer 2003 climate anomaly: A joint flux tower, remote sensing and modelling analysis. *Glob Change Biol*, 13: 634–651
- Richardson A D, Andy Black T, Ciais P, Delbart N, Friedl M A, Gobron N, Hollinger D Y, Kutsch W L, Longdoz B, Luyssaert S, Migliavacca M, Montagnani L, William Munger J, Moors E, Piao S, Reibmann C, Reichstein M, Saigusa N, Tomelleri E, Vargas R, Varlagin A. 2010. Influence of spring and autumn phenological transitions on forest ecosystem productivity. *Phil Trans R Soc B*, 365: 3227–3246
- Richardson A D, Keenan T F, Migliavacca M, Ryu Y, Sonnentag O, Toomey M. 2013. Climate change, phenology, and phenological control of vegetation feedbacks to the climate system. *Agric For Meteorol*, 169: 156–173
- Running S W, Nemani R R, Heinsch F A, Zhao M, Reeves M, Hashimoto H. 2004. A continuous satellite-derived measure of global terrestrial primary production. *Bioscience*, 54: 547–560
- Shen M G, Piao S L, Jeong S J, Zhou L M, Zeng Z Z, Ciais P, Chen D, Huang M T. 2015. Evaporative cooling over the tibetan plateau induced by vegetation growth. *Proc Natl Acad Sci USA*, 112: 9299–9304
- Sun S B, Song Z L, Wu Y T, Wu X C, Wang T J, Du W L, Che T, Huang C L, Zhang X J, Ping B, Lin X F, Li P, Yang Y X, Chen B Z. 2018. Spatio-temporal variations in water use efficiency and its drivers in China over the last three decades. *Ecol Indic*, 94: 292–304
- Sun Y, Piao S L, Huang M T, Ciais P, Zeng Z Z, Cheng L, Li X R, Zhang X P, Mao J F, Peng S S. 2016. Global patterns and climate drivers of water-use efficiency in terrestrial ecosystems deduced from satellite-based datasets and carbon cycle models. *Glob Ecol Biogeogr*, 25: 311–323
- Tang X G, Li H P, Desai A R, Nagy Z, Luo J H, Kolb T E, Oliosio A, Xu X B, Yao L, Kutsch W, Pilegaard K, Köstner B, Ammann C. 2015. How is water-use efficiency of terrestrial ecosystems distributed and changing on earth? *Sci Rep*, 4: 7483
- von Arx G, Dobbertin M, Rebetez M. 2012. Spatio-temporal effects of forest canopy on understory microclimate in a long-term experiment in switzerland. *Agric For Meteorol*, 166-167: 144–155
- Wang H J, Dai J H, Zheng J, Ge Q S. 2015. Temperature sensitivity of plant phenology in temperate and subtropical regions of China from 1850 to 2009. *Int J Climatol*, 35: 913–922
- Wang H J, Zhong S Y, Tao Z X, Dai J H, Ge Q S. 2017. Changes in flowering phenology of woody plants from 1963 to 2014 in North China. *Int J Biometeorol*, doi: 10.1007/s00484-017-1377-2
- Wang H J, Dai J H, Rutishauser T, Gonsamo A, Wu C Y, Ge Q S. 2018. Trends and variability in temperature sensitivity of lilac flowering phenology. *J Geophys Res-Biogeosci*, 123: 807–817
- Wolf S, Keenan T F, Fisher J B, Baldocchi D D, Desai A R, Richardson A D, Scott R L, Law B E, Litvak M E, Brunsell N A, Peters W, van der Laan-Luijkx I T. 2016. Warm spring reduced carbon cycle impact of the 2012 US summer drought. *Proc Natl Acad Sci USA*, 113: 5880–5885
- Wu C Y, Chen J M, Gonsamo A, Price D T, Black T A, Kurz W A. 2012. Interannual variability of net carbon exchange is related to the lag between the end-dates of net carbon uptake and photosynthesis: Evidence from long records at two contrasting forest stands. *Agric For Meteorol*, 164: 29–38
- Wu C Y, Chen J M, Black T A, Price D T, Kurz W A, Desai A R. 2013. Interannual variability of net ecosystem productivity in forests is explained by carbon flux phenology in autumn. *Glob Ecol Biogeogr*, 22: 994–1006
- Yang Y T, Guan H D, Shang S H, Long D, Craig T S. 2014. Toward the use of the modis et product to estimate terrestrial gpp for nonforest ecosystems. *IEEE Geosci Remote Sens Lett*, 11: 1624–1628
- Zhao M S, Heinsch F A, Nemani R R, Running S W. 2005. Improvements of the modis terrestrial gross and net primary production global data set. *Remote Sens Environ*, 95: 164–176
- Zhou S, Yu B F, Huang Y F, Wang G Q. 2014. The effect of vapor pressure deficit on water use efficiency at the subdaily time scale. *Geophys Res Lett*, 41: 5005–5013

Reproduced with permission of copyright owner. Further reproduction prohibited without permission.